Available online at www.sciencedirect.com
SCIENCE DIRECT®
Journal of Catalysis 227 (2004) 175–185
JOURNAL OF CATALYSIS
www.elsevier.com/locate/jcat

A mechanistic approach to phenol methylation on $Cu_{1-x}Co_xFe_2O_4$: FTIR study

Thomas Mathew, Munusamy Vijayaraj, Shivanand Pai, Balkrishna B. Tope, Sooryakant G. Hegde, B.S. Rao, Chinnakonda S. Gopinath *

Catalysis Division, National Chemical Laboratory, Dr. Homi Bhabha Road, Pune 411 008, India

Received 28 May 2004; revised 5 July 2004; accepted 8 July 2004

Available online 5 August 2004

Abstract

The interaction of phenol, methanol, and possible reaction products of phenol methylation with the $Cu_{1-x}Co_xFe_2O_4$ system has been studied by FTIR spectroscopy in the temperature range between 373 and 623 K. The spectra obtained from the chemisorption of methanol onto $Cu_{1-x}Co_xFe_2O_4$ above 373 K indicate progressive oxidation to formate and/or dioxymethylene and then to CO, CO_2, and H_2. Phenol is predominantly adsorbed as phenolate species by the dissociative adsorption on an acid–base site and the phenyl ring of phenol is perpendicular to the catalyst surface, facilitating selective *ortho* methylation by methyl cations. Characteristic ν_{C-O} bands observed for *ortho*-methylated phenols on the catalyst surface allow the identification of the same from the reaction mixture adsorbed on catalysts at 473 K, well below the optimum reaction temperature of 623 K, on Cu-containing catalysts. However, $CoFe_2O_4$ shows little interaction of phenol with MeOH, when they are coadsorbed, and might be a limiting factor to the overall reaction. Coadsorption of acidity probes with phenol and methanol indicates that the same acid–base sites are responsible for the reaction. Methylated phenols show a weak interaction with the surface compared to phenol and are susceptible to desorption at reaction temperatures and thus facilitate efficient methylation.

Keywords: $Cu_{1-x}Co_xFe_2O_4$; Phenol; Methylation; *o*-Cresol; 2,6-Xylenol; DRIFT; Adsorbate interaction; Reaction mechanism; Acid–base pair; IR

1. Introduction

Methylation of phenol with methanol results in a range of products such as anisole, *o*-cresol, *p*-cresol, and dimethyl phenols including 2,6-xylenol, which are important intermediates in the production of agrochemicals, pharmaceuticals, and polymer [1,2]. A thorough literature survey of phenol methylation [3–20] revealed that there is a competition between O- and C-methylation and the acid–base properties of the system play an important role in the product selectivity besides experimental factors. It is to be noted that Fe_2O_3 in combination with other oxides such as CdO, SnO_2, CeO_2, NiO, CoO, Cr_2O_3, and ZrO_2 show high selectivity to *ortho* methylation [13–18].

Although there have been many reports on the catalytic activity for phenol methylation on various systems, spectroscopic data on the interaction of phenol, methanol, and their products with solid catalysts are scarce for understanding the mechanistic aspects of the reaction. IR techniques are ideally suited for investigating the nature of adsorbed intermediates in situ on the oxide surfaces. The spectra of adsorbed species provide information of any chemical changes that occur on the surface. Kotanigawa and co-workers [16–18] studied the adsorption behavior of phenol and methanol on a $ZnO–Fe_2O_3$ system and highlighted the importance of acid–base sites for the selective *ortho* methylation. However, a detailed study of the adsorption behavior of possible products and reactants of phenol methylation on catalytic systems is not available to date.

Our earlier investigations [19–22] on the kinetic, catalytic, and spectroscopic aspects of the methylation of phe-

* Corresponding author. Fax: 0091-20-2589 3761.
E-mail address: gopi@cata.ncl.res.in (C.S. Gopinath).

0021-9517/$ – see front matter
doi:10.1016/j.jcat.2004.07.005

nol on $Cu_{1-x}Co_xFe_2O_4$ system revealed that these catalysts are more efficient compared to other catalysts studied for the synthesis of *o*-cresol and 2,6-xylenol. Here we report the FTIR study of the adsorption of phenol, methanol, coadsorption of phenol + methanol, HCHO, HCOOH, and possible products like anisole, *o*-cresol and 2,6-xylenol on a $Cu_{1-x}Co_xFe_2O_4$ system to understand the interaction of the above compounds and to gain insight on the mechanism of phenol methylation. The FTIR results are also discussed in relation to the catalytic data.

2. Experimental

$Cu_{1-x}Co_xFe_2O_4$ ($x = 0$, 0.25, 0.50, 0.75, and 1) samples were prepared by a coprecipitation technique and characterized by various physicochemical techniques as reported in our earlier publications [19–21]. FTIR spectra of the ferrite samples were recorded on a Shimadzu 8300 spectrometer equipped with a MCT-A detector. IR studies of any of the reactant-, product-, and pyridine-adsorbed samples were recorded in diffuse reflectance infrared Fourier transform spectroscopy (DRIFTS) mode. Calcined powder sample was taken in a sample holder and placed in SpectraTech-made DRIFTS cell with a ZnSe window (Model 0030-067). Water circulation of ZnSe window keeps the temperature below 323 K even at a catalyst temperature of 573 K. The DRIFTS cell is equipped with an inlet and an outlet to introduce the probe molecules in a nitrogen stream and the vaporized molecules are adsorbed on the catalyst. The samples were then heated in situ from room temperature to 673 K at a heating rate of 5 K/min in a flowing stream (40 ml/min) of 99.99% pure N_2. The sample was kept at 673 K for 3 h and then the hydroxyl region of the spectra was measured. The sample was then cooled to 373 K and vapors of phenol, methanol, and the other reaction products were introduced into the N_2 flow as noted above for 10 min. Since 2,6-xylenol is solid at room temperature, it was dissolved in CCl_4 and warmed to 318 K and introduced in the N_2 flow. C–Cl vibrations do not interfere in the IR region of interest reported here and CCl_4 is vaporized below 373 K also. After adsorption of reactant(s) or product the IR spectra were recorded at 373 K and then the catalyst temperature was slowly increased under the N_2 flow and spectra were recorded at different temperatures up to 673 K. A resolution of 4 cm^{-1} was attained after averaging over 500 scans for all the IR spectra reported here. All spectra are presented here as the difference spectra between the molecule adsorbed on catalyst and pure catalyst surfaces. Except for hydroxyl species, there is no IR band observed between 3500 and 1000 cm^{-1} on catalyst surfaces.

3. Results

3.1. Adsorption of methanol

FTIR spectra of methanol (bottom three traces) adsorbed on three selected catalyst compositions ($x = 0$, 0.5, and 1) at different temperatures were recorded and shown in Fig. 1 along with HCHO and HCOOH (top two traces) adsorbed on $Cu_{0.5}Co_{0.5}Fe_2O_4$ at temperatures between 373 and 623 K. Bands around 2940, 2924, 2816, 1460, 1370, 1060, and 1030 cm^{-1} characterize the typical surface methoxy groups

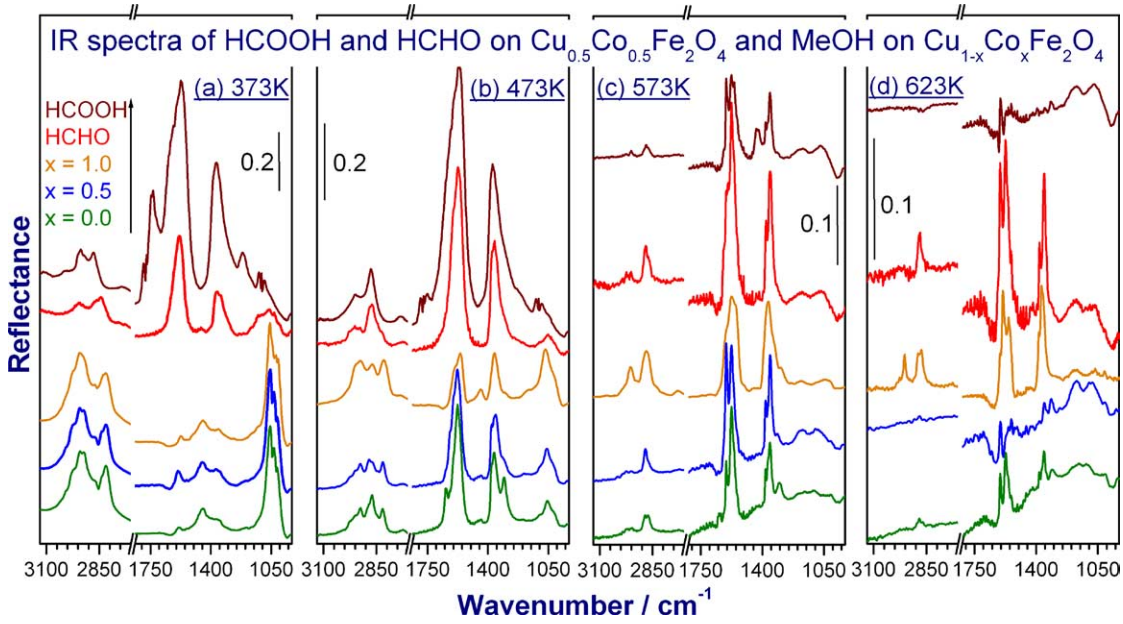

Fig. 1. Temperature-dependent FTIR spectra of methanol adsorbed on $Cu_{1-x}Co_xFe_2O_4$ for three selected catalyst compositions of $x = 0.0$, 0.5, and 1 at (a) 373, (b) 473, (c) 573, and (d) 623 K. IR spectra of HCOOH and HCHO adsorbed on $Cu_{0.5}Co_{0.5}Fe_2O_4$ at different temperatures are also shown for reference in the top two traces.

Table 1
Bands corresponding to (a) methoxy and (b) formate species obtained from the FTIR by the adsorption of methanol on $Cu_{1-x}Co_xFe_2O_4$ and variety of supports (from the literature)

(a) Methoxy

Assignment	MeOH gas phase	Al_2O_3	V–Ti–O	TiO_2	Fe_2O_3	Present studies on $Cu_{1-x}Co_xFe_2O_4$		
	Refs. [33,36]	Ref. [26]	Ref. [35]	Ref. [24]	Ref. [23]	$x = 0.0$	$x = 0.5$	$x = 1.0$
$\nu_{as}(CH_3)$	2962	2970	2965	2965	–	2940	2941	2942
$\nu_s(CH_3)$	–	2955	2935	2930	2920	2922	2921	2926
$2\delta_s(CH_3)$	2844	2844	2830	2830	2815	2818	2816	2818
$\delta_{as}(CH_3)$	1455	1472	1452	1462	1460	1460	1450	1460
$\delta_s(CH_3)$	–	1458	1438	1436	1440	1440	1437	1445
$r(CH_3)$	1150	1200	1150	1151	–	–	–	–
$\nu(CO)$	1034	1095	< 1080	1125	–	1055	1055	1060
$\delta(COH)$	1340	–	1370	1370	–	–	–	–

(b) Formate

Assignment	$ZnAl_2O_4$	ZnO	V–Ti–O	TiO_2	Fe_2O_3	Present studies on $Cu_{1-x}Co_xFe_2O_4$		
	Ref. [37]	Ref. [37]	Ref. [35]	Ref. [24]	Ref. [23]	$x = 0.0$	$x = 0.5$	$x = 1.0$
$\nu_{as}(COO^-) + \delta(CH)$	2970	2960	2972	2970, 2950	–	2976	2972	2975
$\nu(CH)$	2900	2882	2883	2885, 2870	2880	2887, 2870	2884, 2867	2889 2873
$\nu_s(COO^-) + \delta(CH)$	2770	2740	–	–	–	–	–	–
$\delta_{as}(COO^-)$	1590	1580	1565, 1540	1575, 1560	1555	1575	1577	1588, 1562
$\delta(CH)$	1395	1382	1378	1390 1380	1376	1375	1378	1377
$\nu_s(COO^-)$	1375	1365	1370 1358	1372 1360	1348	1364	1361	1360

due to MeOH adsorption at 373 K [23–35]. The various bands due to methanol adsorption on $x = 0$, 0.5, and 1 and their assignments are summarized in Table 1a along with the literature data on relevant supports. Bands due to CH_3 of OCH_3 are observed at ~ 2945 cm^{-1} ($\nu_s(CH_3)$) and 2816 cm^{-1} ($2\delta_s(CH_3)$) and they are in Fermi resonance with each other [24]. The presence of OCH_3 species during methanol oxidation is indicated by C–O stretching mode at 1060 cm^{-1} [23–27]. Other low-frequency symmetric and asymmetric methyl bands appear as low intensity shoulders at ~ 1440 and ~ 1460 cm^{-1}. A comparison of MeOH adsorbed on different catalyst compositions at 373 K reveals that there is no significant difference among them.

Vibrations due to HCHO and HCOOH species are also observed due to methanol adsorption at temperatures higher than 373 K at 2952, 2875, 1570, 1375, and 1365 cm^{-1} [23–35]. All these bands are well assigned and in good correspondence with the HCHO and HCOOH adsorbed on $x = 0.5$ and literature values, summarized in Table 1b. The band observed at 2975 cm^{-1} is due to the Fermi resonance vibration of both asymmetric COO^- stretching and CH deformation [24]. Adsorption of HCOOH and HCHO separately on $x = 0.5$ enables the differentiation of formate and methoxy species formed on the surface of these oxides; however, both HCHO and HCOOH show vibrations at comparable frequencies due to similar carbonyl and C–H stretchings, indicating that it would be difficult to distinguish the formation of the above species on catalyst surfaces at 473 K. HCOOH and HCHO on $x = 0.5$ display bands around 2950, 2876, 1570, 1370, and 1360 cm^{-1} (Fig. 1b). These species can readily be identified as formate ions, assigning the peak maximum at 2877, 1576, 1370, and 1360 cm^{-1}, respectively to C–H stretching, COO^- asymmetric stretching, C–H deformation, and COO^- symmetric stretching vibrations [23–25]. The difference between HCHO and HCOOH-adsorbed surfaces becomes very clear at 573 K due to the equal intensity doublet peaks around 1585 cm^{-1} for the latter than the former. Similar formate species were detected on adsorption of HCOOH on Fe_2O_3 [23,28], V–Ti oxides [24], and other oxides [29–32]. Thus the spectroscopic features of formate species produced by HCOOH are similar to those of CH_3OH and indicate that the CH_3OH oxidation proceeds via a formate intermediate.

Reasonably strong bands are observed at 1645 and 1309 cm^{-1} on $x = 0$ and 0.5 due to HCHO and in correspondence with adsorbed HCHO on $x = 0.5$ at 473 K [23,25]; however, on $x = 1$ the intensity of these bands decreases considerably. A weak band at 1622 cm^{-1} is assigned to coordinatively bonded species through the carbonyl oxygen to Lewis acid sites [23].

Heat treatment of MeOH-adsorbed catalysts above 373 K causes a considerable decrease in the intensity of bands associated with OMe species; however, the formate species at 2950, 2883, 2863, 1583, 1375, and 1360 cm^{-1} grows in intensity (Fig. 1b). Similar observations have already been detected on various oxides such as Fe_2O_3 [23], TiO_2

[24,27], SnO_2 [32], ZrO_2 [34], V_2O_5 [34,35], and Cr_2O_3 [38]. However, the shifts observed on $Cu_{1-x}Co_xFe_2O_4$ in comparison with the single component oxides are significant to conclude that species formed on $Cu_{1-x}Co_xFe_2O_4$ are indeed characteristic of a mixed phase. Splitting and reduction in intensity of several bands $\geqslant 473$ K indicate that adsorbed MeOH undergoes chemical changes of oxidation on $Cu_{1-x}Co_xFe_2O_4$.

The adsorption behavior of CH_3OH on $Cu_{1-x}Co_xFe_2O_4$ showing notable differences between Cu-containing samples ($x < 1$) and $CoFe_2O_4$ consists of the following: (1) The intensity of adsorbed species at 473 K on $x = 1$ is relatively low compared to $x < 1$ and indicates that a high temperature is necessary for the activation of MeOH on $x = 1$; (2) The relative concentration of OCH_3 species increases with x at 473 K and a small amount persists even at 573 K on $x = 1$. Contrarily, the intensity of formate species increased to a considerable extent at 473 K on $x < 1$ compositions. This shows that MeOH is susceptible to oxidation on $x < 1$ at lower temperatures than on $CoFe_2O_4$.

It is clearly evident that at 573 K, MeOH is oxidized to HCOOH on $x = 0.5$ and mostly HCHO on $x = 0$ and 1. Very good resemblance between MeOH or HCHO/HCOOH adsorbed on catalysts at 573 K supports the above point. Further new features observed at 1178 and 1070 cm^{-1} indicate the formation of dioxymethylene (DOM) [24] in all three cases of HCHO, HCOOH, and MeOH adsorbed on the $x = 0.5$ composition; however, the DOM features are not apparent on $x = 0$ and 1. Further heating to 623 K leads to desorption of HCOOH on $x = 0.5$; however, some DOM remains on the surface. $x = 0$ and 1 resembles that of adsorbed HCHO and HCOOH features, respectively. A mere decrease in intensity of the HCHO features on $x = 0$ from 573 to 623 K suggests its desorption. Note the resemblance between MeOH on $x = 1$ at 623 K and HCOOH on $x = 0.5$ at 573 K. Formate species are somewhat stable on $x = 1$ even at 623 K; whereas both the above species are hardly found on $x < 1$ samples at 623 K, indicating that MeOH is mostly reacted on $x < 1$ spinel surfaces to CO, CO_2, and H_2. Finally, C–H stretching vibrations are observed up to 623 K with relatively high intensity on $x = 1$.

3.2. Adsorption of phenol

Fig. 2 shows the temperature-dependent FTIR spectra of phenol adsorbed on $Cu_{1-x}Co_xFe_2O_4$ ($x =$ (a) 0, (b) 0.5, and (c) 1), between 373 and 623 K. Strong bands at 1587, 1485, and 1256 cm^{-1} are observed due to phenol adsorption. The band and shoulder at 1587 and 1595 cm^{-1} (clear at 473 K) are assigned to ν_{8a} and ν_{8b} deformation vibrations of the aromatic ring, respectively [39,40]. These bands are displaced to lower ν as compared to bands at 1604 and 1596 cm^{-1} phenol in CCl_4 [40]. The single broad intense band observed at 1485 cm^{-1} at 373 K is resolved into two components at 1485 and 1473 cm^{-1} at higher temperatures ascribed to normal modes ν_{19a} and ν_{19b} of the aromatic

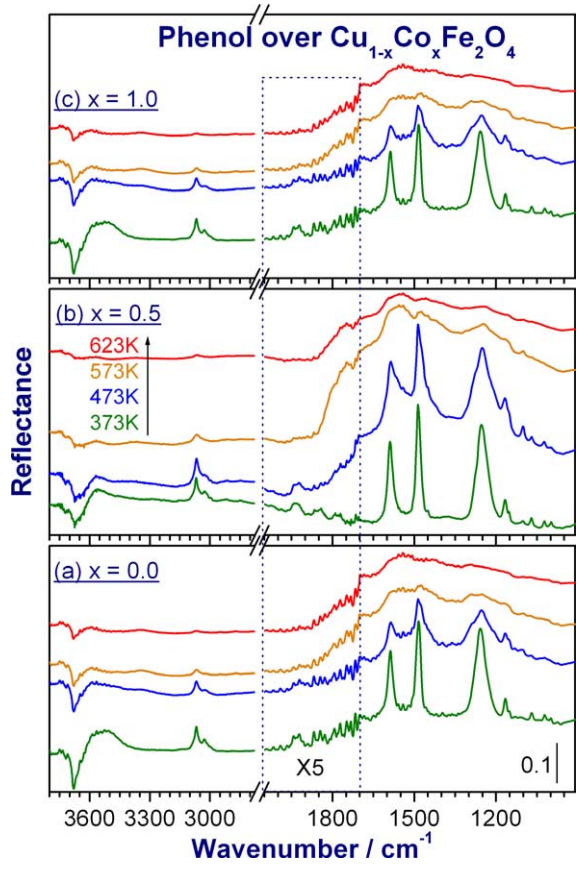

Fig. 2. Temperature-dependent FTIR spectra of phenol adsorbed on $Cu_{1-x}Co_xFe_2O_4$ for three selected catalyst compositions of (a) $x = 0.0$, (b) 0.5, and (c) 1.0. Intensity scale is same in all panels. Note: the 2050–1700 cm^{-1} region is multiplied by a factor of 5 to show the features clearly.

ring. The intense broad band at 1255 cm^{-1} is due to C–O stretching vibration. A reasonable intensity C–O–H bending fundamental band appears at 1166 cm^{-1} for all catalyst compositions up to 473 K. The presence of a series of definite low-intensity bands along with sizeable intensity bands at 1930, 1850, and 1780 cm^{-1} is due to out-of-plane aromatic C–H bending in the region 2050–1700 cm^{-1} and is an indication of perpendicular orientation of phenol over these oxides [41]. The spectrum in the C–H stretching region shows absorption maxima at 3068 and 3025 cm^{-1}, which is typical of the C–H stretching vibration of the aromatic ring of phenol. A series of bands observed between 4000 and 3400 cm^{-1} and 1750 and 1540 cm^{-1} indicates the phenolic O–H stretching as well as stretching vibration of O–H due to the dissociative adsorption of phenol.

Heating to 473 K and above leads to a depletion of band intensity at 1587, 1485, and 1255 cm^{-1} and splitting into several low-intensity components. It is to be noted that approximately 80–90% of the band intensity observed at 373 K is retained on $x = 0.5$ at 473 K too; however the band intensity decreases to 50% on $x = 0$ and 1 at 473 K. The band at 1587 cm^{-1} is shifted to 1582 cm^{-1} and the shoulder associated with this band is well resolved at 473 K and appears at

1596 cm^{-1}. An apparent single peak at 1485 cm^{-1} at 373 K starts splitting into two components at 1473 and 1485 cm^{-1} at 473 K and grows as separate peaks on further increase of temperature. The broad band at 1255 cm^{-1} corresponding to ν_{C-O} vibration is clearly split into two low-intensity components, indicating the formation of different phenolic species on $Cu_{1-x}Co_xFe_2O_4$. The appearance of ν_{C-O} band at 1288 cm^{-1} at 473 K is indicative of deprotonated phenol, in which the C–O bond is further strengthened. A high-frequency shift of the ν_{C-O} vibration has been reported for phenolate in basic aqueous solution [42,43].

On increasing the temperature to $\geqslant$ 573 K, an overall broadening of peaks is observed; nonetheless the $x = 0.5$ composition shows relatively intense peaks than other compositions. There is a good similarity among $x = 0$ and 1 compositions, especially in the 3800–3550 cm^{-1} (OH_{str}) and 2050–1700 cm^{-1} regimes; however, the $x = 0.5$ composition shows a fast depleting intensity. Further the noise level is high for $x = 0$ and 1 in the overtone regime than $x = 0.5$. The ν_{C-O} band at 1288 cm^{-1} is weak on $x = 0.5$ than the other compositions. The above observations suggest that desorption of phenolic species is fast $>$ 473 K on $x = 0.5$ and there is a gradual desorption with increasing temperature on other compositions.

3.3. Adsorption of anisole

Fig. 3 shows the temperature-dependent FTIR spectra of anisole adsorbed on $Cu_{0.5}Co_{0.5}Fe_2O_4$. In the region of aromatic ring (C=C) vibrations (top panel) prominent peaks are observed at 373 K at 1594 and 1493 cm^{-1}. Corresponding peaks for liquid anisole are at 1600 and 1500 cm^{-1} [47], indicating that anisole is weakly bonded to the surface. At least three overlapping bands are observed between 1080 and 1000 cm^{-1}, indicating the presence of H_3C–O vibrations of anisole. The major peak at 1242 cm^{-1} is due to ν_{C-O} of C_6H_5–O vibrations; however, another ν_{C-O} observed at 1290 cm^{-1} with reasonable intensity indicates that there could be dissociation of anisole to some extent and hence phenoxide formation. Low-frequency symmetric and asymmetric methyl bands appear at 1447 and $\sim$ 1465 cm^{-1} and it is likely that aromatic C=C vibration ν_{19b} overlaps with the above bands. Bands detected in the range 2050–1700 cm^{-1} indicate that the orientation of the aromatic ring is perpendicular to the surface. Bands at 3062 and 3008 cm^{-1} are due to ν_{C-H} of the aromatic ring (Fig. 3, bottom panel). Additional vibrations observed at 2947, 2922, 2840, and 2810 cm^{-1} are due to the CH_3 group of anisole. On increasing the temperature to 473 K, some important variations of these peaks are observed. ν_{C-O} intensity at 1242 cm^{-1} decreases and this is in contrast to the observation of phenol on $x = 0.5$ at 473 K. Clear $C–H_{def}$ peaks of methyl group appear at 1375 and 1355 cm^{-1} and the methyl band intensity decreases around 1460 cm^{-1}. A corresponding change in the $C–H_{str}$ regime shows a peak at 2880 cm^{-1} and further supports the dissociation of methyl groups from anisole.

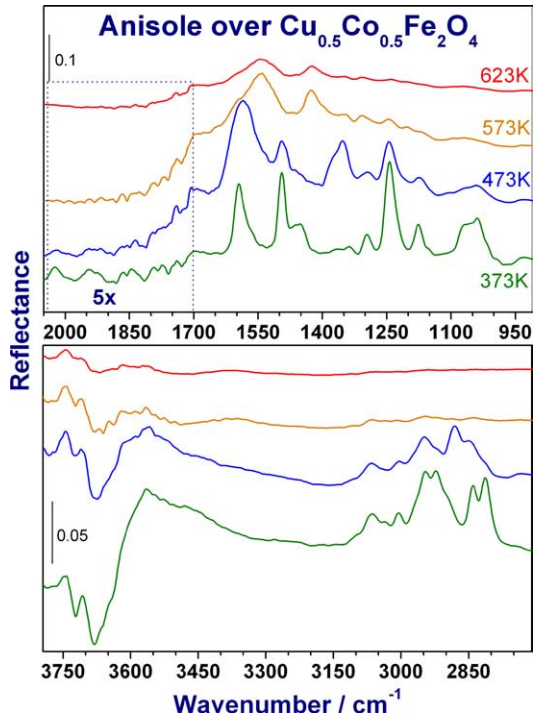

Fig. 3. Temperature-dependent FTIR spectra of anisole adsorbed on $Cu_{0.5}Co_{0.5}Fe_2O_4$ in the range of 2050–900 cm^{-1} (top panel) and 3800–2700 cm^{-1} (bottom panel). Note: the 2050–1700 cm^{-1} region is multiplied by a factor of 5 to show the features clearly.

Above 473 K, no out-of-plane aromatic C–H bending peaks are observed, indicating a change in orientation of anisole molecules from perpendicular to parallel (or tilted) toward the surface. A shift in the frequency of bands and negative bands confirm the weak interaction of anisole with the catalyst surface and the fast desorption from the surface as the temperature increases.

3.4. Adsorption of *o*-cresol

Fig. 4 shows FTIR spectra of *o*-cresol adsorbed on $Cu_{0.5}Co_{0.5}Fe_2O_4$ at different temperatures. The above spectra are almost similar to those of adsorbed phenol with some changes. The spectra show major bands at 1615, 1593, 1575, 1483, and around 1450 cm^{-1} due to aromatic ring vibrations. The splitting observed with the above aromatic vibrations are typical for *o*-cresol and attributed to ν_{8a}, ν_{8b}, ν_{19a}, and ν_{19b}. However, the intensity of the above aromatic vibrations is significantly low compared to that of phenol and indicates its interaction with the catalyst surface is low. The broad band observed at 1248 cm^{-1} with two shoulders at 1270 and 1292 cm^{-1} is due to the stretching vibration of the C–O bond. The low intense band observed at 1375 cm^{-1} is due to the symmetrical bending mode vibration of the CH_3 group. Symmetric and asymmetric methyl group bands are observed at 1445 and 1460 cm^{-1}, respectively. Like phenol, adsorption of *o*-cresol also produces bands in the range 2050–1700 cm^{-1} with a clear broad band at 1900 cm^{-1} at all temperatures studied. The above observations lead to a

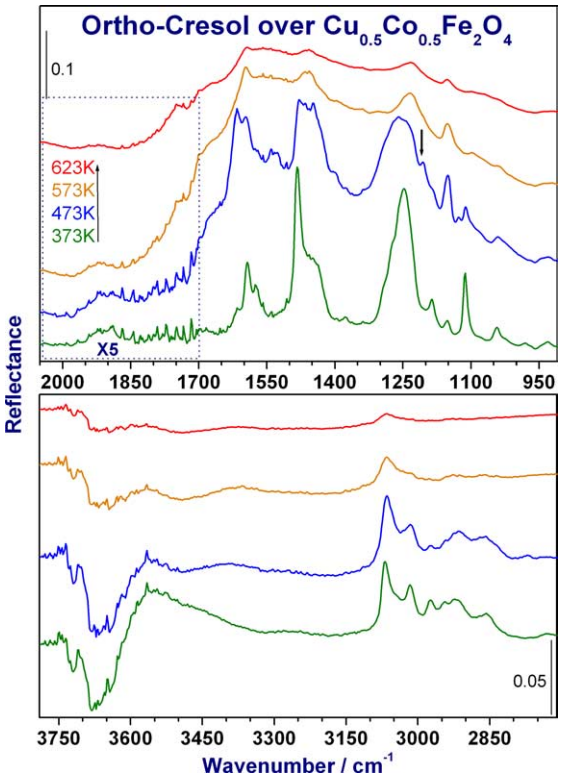

Fig. 4. Temperature-dependent FTIR spectra of *ortho*-cresol adsorbed on $Cu_{0.5}Co_{0.5}Fe_2O_4$ in the range of 2050–900 cm^{-1} (top panel) and 3800–2700 cm^{-1} (bottom panel). Note: the 2050–1700 cm^{-1} region is multiplied by a factor of 5 to show the features clearly.

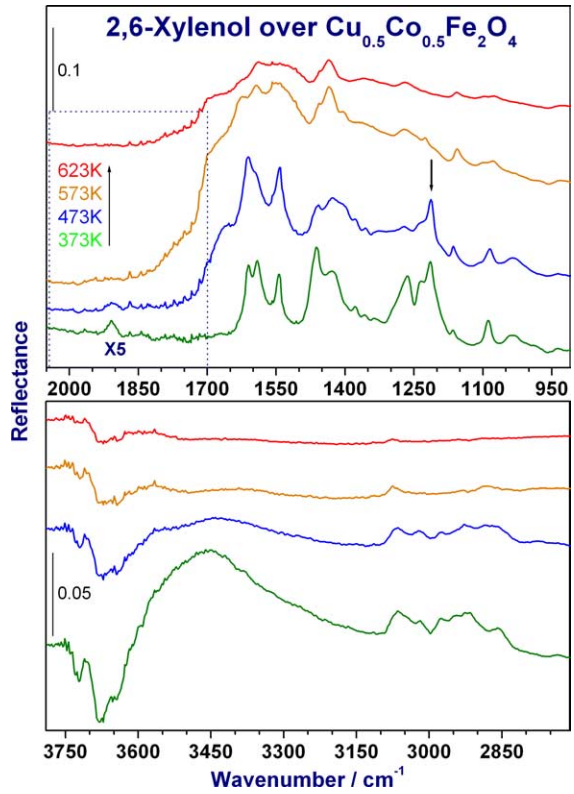

Fig. 5. Temperature-dependent FTIR spectra of 2,6-xylenol adsorbed on $Cu_{0.5}Co_{0.5}Fe_2O_4$ in the range of 2050–900 cm^{-1} (top panel) and 3800–2700 cm^{-1} (bottom panel). Note: the 2050–1700 cm^{-1} region is multiplied by a factor of 5 to show the features clearly.

conclusion that the aromatic ring of *o*-cresol is perpendicular to the catalyst surface. The bands observed between 2980 and 2850 cm^{-1} are attributed to the vibrations of CH_3 group of *o*-cresol. OH stretching vibrations observed for *o*-cresol between 3800 and 3400 cm^{-1} are comparable to those of phenol (Fig. 2) on $x = 0.5$. An increase in temperature to $\geqslant 473$ K, generally, depletes the intensity of all the bands. However, the intensity of ν_{C-O} band is slightly higher than the intensity of various aromatic ring vibrations, indicating the high strength of adsorption through oxygen atoms. Further a new ν_{C-O} band appears at 1207 cm^{-1}. The ν_{C-O} band shifts significantly to 1230 cm^{-1} with the new ν_{C-O} band still present at 573 K. Though the intensity of all the peaks decreases as the temperature increases, a majority of the bands persist even at 623 K, suggesting that *o*-cresol is still bound significantly with the aromatic ring perpendicular to the surface.

3.5. Adsorption of 2,6-xylenol

FTIR spectra of 2,6-xylenol adsorbed on $Cu_{0.5}Co_{0.5}Fe_2O_4$ at different temperatures are shown in Fig. 5. Adsorption of 2,6-xylenol at 373 K on $x = 0.5$ produces a doublet in the aromatic region around 1600 and another feature at 1543 cm^{-1} due to the aromatic ring stretching vibrations ν_{8b} and ν_{8a}, respectively. The bands observed at 1483 and 1450 cm^{-1} are attributed to the aromatic ring vibrations ν_{19a} and ν_{19b}, respectively. Unlike *o*-cresol, the band at 1375 and 1355 cm^{-1} is clear due to bending vibration modes of CH_3 groups in 2,6-xylenol. Unlike phenol and *o*-cresol, the intensity of ν_{C-O} stretching band decreased considerably and shifted to 1232 cm^{-1}, suggesting the weak interaction of 2,6-xylenol with the catalyst surface. Additionally ν_{C-O} bands with comparable intensity are observed at 1264 and 1212 cm^{-1} also at 373 K. It is also to be noted that the aromatic ring vibrations around 1600 cm^{-1} are higher in intensity compared to the band at 1543 cm^{-1}. Bands around 1600 cm^{-1} are equal in intensity and are attributed to the high symmetry of 2,6-xylenol than a triplet with different intensity for *o*-cresol. Symmetric and asymmetric methyl group bands are observed at 1460 and 1430 cm^{-1}, respectively, with good intensity. Bands at 1910, 1840, and 1780 cm^{-1} with definite intensity and other low-intensity features between 2050 and 1700 cm^{-1} indicate that the aromatic ring of 2,6-xylenol is perpendicular to the catalyst surface. The bands due to CH_3 groups appear at 2974, 2950, 2930, 2870, and 2855 cm^{-1}, and aromatic C–H stretching is observed at 3066 and 3020 cm^{-1}.

Increase in temperature generally decreases the intensity of all the peaks and indicates that the interaction with the surface decreases rapidly. However, aromatic ring vibrations and the ν_{C-O} band at 1210 cm^{-1} remain high in intensity at 473 K. The above peak is to be compared to a

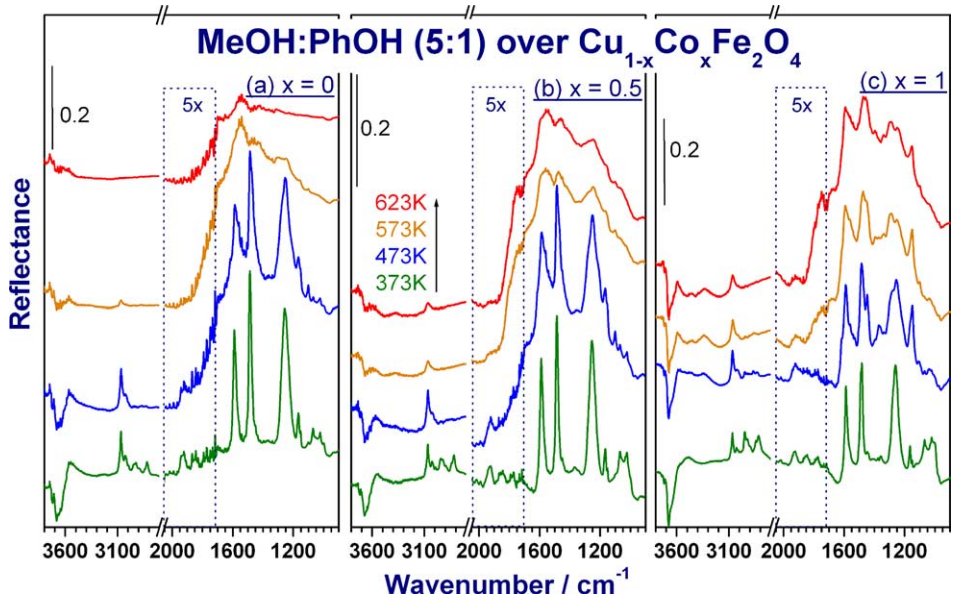

Fig. 6. Temperature-dependent FTIR spectra of phenol to methanol of 1:5 mole ratio coadsorbed on $Cu_{1-x}Co_xFe_2O_4$ system. (a) $x = 0.0$, (b) $x = 0.5$, and (c) $x = 1.0$. Note: the 2050–1700 cm^{-1} region is multiplied by a factor of 5 to show the features clearly.

similar peak in *o*-cresol at 1207 cm^{-1} and hints that this peak is very specific for *ortho*-methylated phenols. A further rise in temperature ($\geqslant$ 573 K) decreases the intensity of the overall spectrum, indicating the desorption of 2,6-xylenol. Thus, 2,6-xylenol desorbs fast from the surface $\geqslant$ 473 K than *o*-cresol or phenol. Increase in temperature does not cause any change in peak positions.

3.6. Coadsorption of phenol and methanol

Fig. 6 shows the temperature-dependent FTIR spectra of $Cu_{1-x}Co_xFe_2O_4$ catalysts exposed to 1:5 mole ratio of phenol:methanol at 373 K and subsequently heated up to 623 K. Very interesting features observed due to the above reaction mixture change with temperature and catalyst composition too. The main points worth highlighting from the coadsorption of phenol and methanol are as follows. (a) First, phenol features dominate all the catalyst surfaces despite a low phenol content in the reaction mixture. (b) Low-intensity ν_{C-O} bands of methoxy moieties are observed around 1067 cm^{-1} at 373 K, and its intensity increases with increasing Co content on the catalyst. However, the methoxy moiety disappears at 473 K on $x < 1$, and a weak band on $x = 1$. (c) No bands due to formate or HCHO or DOM species due to MeOH oxidation were observed at any temperature on any catalyst composition, demonstrating that the MeOH oxidation is prohibited in the presence of phenol. (d) ν_{C-H} stretching vibrations due to MeOH disappear mostly at 473 K on $x < 1$, but at 573 K on $x = 1$. Similarly, ν_{C-H} stretching vibrations of phenol disappear with increasing temperature on $x < 1$; however, the intensity of the above band at any temperature increases with Co content. Further $x = 1$ does not show considerable desorption of phenol up to 623 K. (e) A sharp ν_{C-O} band appearing at 1250 cm^{-1} at 373 K on all catalyst compositions broadens at high temperatures on $x < 1$ and a shoulder, characteristic of *ortho*-methylated phenols, is visible around 1210 cm^{-1}; note the large valley between bands at 1250 and 1166 cm^{-1} on $x = 1$ and a distinct shoulder at 1280 cm^{-1} at 473 K. (f) A new ν_{O-H} stretching band appears around 3340 cm^{-1} on $x = 1$ at 473 K and increases in intensity at 573 K; such a band appears on $x = 0.5$ with weak intensity and no band at 3340 cm^{-1} on $x = 0$ indicates that this band is somewhat specific to cobalt ions. (g) The C–O–H bending band at 1166 cm^{-1} disappears < 573 K on $x < 1$; however, it strongly persists on $x = 1$ at 623 K; $O-H_{str}$ bands also persists at 623 K on $x = 1$ and disappear gradually with increasing temperature for $x < 1$. (h) The aromatic ring vibration of phenol at 1585 cm^{-1} is shifted to 1593 cm^{-1} and exhibits a shoulder at 1570 cm^{-1}. The narrow band at 1481 cm^{-1} observed on phenol adsorption is shifted to 1487 cm^{-1} and overlapped with an additional band at 1472 cm^{-1}. The above four bands are characteristic bands of *o*-cresol and 2,6-xylenol. (j) Out-of-plane C–H (overtone) vibrations between 2050 and 1700 cm^{-1} are seen nicely for all catalyst compositions; however, it disappears for $x = 0$ and 0.5 at > 473 and > 573 K, respectively; It remains observed on $x = 1$ at 623 K. All the above points hint that the coadsorption of methanol and phenol leads to a good interaction among them above 373 K on $x < 1$ and there are indications toward methylated product formation at 473 K. Contrarily, $CoFe_2O_4$ indicates a low profile interaction among the reactants, even at 573 K, and in combination with the above points indicates that the phenol dissociation and methyl cation availability could be the limiting factors to the overall methylation reaction; however, the *ortho* methylation step is somewhat fast and occurs at around 473 K on Cu-containing compositions, suggesting the importance of Cu^{2+} in the spinels.

4. Discussion

4.1. Reactivity of methanol on $Cu_{1-x}Co_xFe_2O_4$

A comparison of the IR spectra of CH_3OH, HCHO and HCOOH (Fig. 1) on $Cu_{1-x}Co_xFe_2O_4$ reveals methoxylation on the surface and subsequent oxidation. A likely mechanism for methoxy formation on the surface of oxides is given below [32,44]:

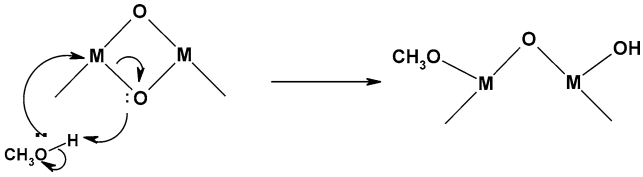

Pyridine adsorption also demonstrates a trace amount of Brønsted acid sites on catalysts [21] and no molecular water is produced during methanol chemisorption. This supports that the most likely mechanism is dissociative chemisorption. Methoxy species on oxide surfaces are progressively converted to formate species > 373 K and indicate that the catalytic oxides are reactive toward methanol. However $x = 0.5$ shows a direct oxidation to DOM through an intermediate of formic acid. $x = 0$ indicates the oxidation to HCHO at 623 K and no evidence of HCOOH/DOM was observed. $x = 1$ composition shows the oxidation to formic acid at 623 K through HCHO. However, all catalyst compositions oxidize methanol to typical reformate products above 573 K, which is confirmed by products analysis. Photoemission and X-ray diffraction analyses of spent catalysts also show that the presence of Cu and Cu^+ and the amount of reduced Cu species increases with Cu content [19]. Further, the formate concentration in the case of Cu-containing spinels is higher than that of $CoFe_2O_4$ indicating that the presence of Cu has a promoting role in their formation [37]. Relatively high concentrations of formate species on $CoFe_2O_4$ at 623 K indicate its stability. Although all the catalyst compositions show a general trend toward methanol adsorption and subsequent oxidation, the small amount of methoxy species observed at 573 K and reasonable amount of formate species seen on $x = 1$ at 623 K suggest that methanol seems activated only at high temperatures on $CoFe_2O_4$. Kinetic data on the *ortho* methylation of phenol also leads to the same conclusion that, unlike Cu-containing compounds, $CoFe_2O_4$ shows high phenol conversion and *ortho*-methylated phenol selectivity at 648–673 K, whereas for Cu-containing catalysts it is at 623 K [19].

4.2. Reactivity of phenol and phenolic products on $Cu_{1-x}Co_xFe_2O_4$

IR studies of adsorption of phenol on $Cu_{1-x}Co_xFe_2O_4$ show both phenol and phenolate-like species. Phenolate species are formed due to the dissociative adsorption of phenol on an acid–base pair site. Phenolate ion is adsorbed on a metal cation (Lewis acid site) whereas the dissociated H^+ on a nearby oxide ion. Thus a series of O–H bands are formed in the range of 4000 and 3400 cm^{-1} (Fig. 2).

A close examination of bands in the region 2050–1700 cm^{-1} for phenol and methylated phenols reveals a number of low-intensity out-of-plane combination bands [41]; however, these bands appear for phenol as well as methylated phenols. It is also known that chemisorbed aromatic molecules with the plane of the aromatic ring parallel to the adsorbent surface lead to a loss in the intensity of out-of-plane C–H vibrations [45,46,48]. When the aromatic ring of PhOH molecule is perpendicular to the surface the out-of-plane C–H ring vibration can be observed, as there is no interaction with the surface. Our recent IR study of N-methylation of aniline with methanol on $Cu_{1-x}Zn_xFe_2O_4$ [49] also supports the above conclusion. In the case of the aromatic ring parallel to the surface and its interaction to the surface through a phenyl ring, the above vibrations are severely restricted as it is very close to the surface and hence those bands are not observed in IR [41,45,46,48,49]. From the above points, it is concluded that the phenol and methylated phenol molecules are adsorbed through O atoms to the Lewis acid sites whose aromatic ring is perpendicular or nearly perpendicular to the plane of the oxide.

This situation is quite similar in the case of coadsorption of phenol and methanol. Methanol is adsorbed onto the protons released by phenol, which in turn interact with the *ortho* position of the phenol, as shown in Fig. 7 [50]. This interaction governs the orientation of the aromatic ring of phenol and the presence of bands in the range 2050–1700 cm^{-1} suggests that the aromatic ring of phenol is almost perpendicular to the surface while interacting with methanol. From the above, it is apparent that the *meta* and *para* positions are far removed from the surface, and further supported the absence of *meta*- and/or *para*-methylated products [19,50]. The adsorption state of *o*-cresol and 2,6-xylenol supports the above points.

The ν_{C-O} bands for chemisorbed methyl phenols show a characteristic stretching at 1210 cm^{-1}, which is not at all observed for phenols. The nature and appearance of the above ν_{C-O} band for phenol in the presence of methanol at 473 K are similar to those of *o*-cresol and 2,6-xylenol. The intensity of aromatic C–H stretching vibrations decreases in intensity as expected from phenol to *o*-cresol to 2,6-xylenol, as the number of such C–H bonds decreases; however, methyl group stretching vibrations do not show any change in intensity between *o*-cresol and 2,6-xylenol. Generally, as the number of CH_3 group increases the overall intensity of various bands decreases considerably compared to phenol, which indicates that the interaction of *ortho*-methylated products interaction with the catalyst surface decreases from phenol to *o*-cresol to 2,6-xylenol and is highly susceptible to desorption at high temperatures. This is an essential requisite for achieving efficient methylation. Thus it is highly plausible that the aromatic rings of these *ortho*-methylated phenols have become somewhat tilted toward the surface at

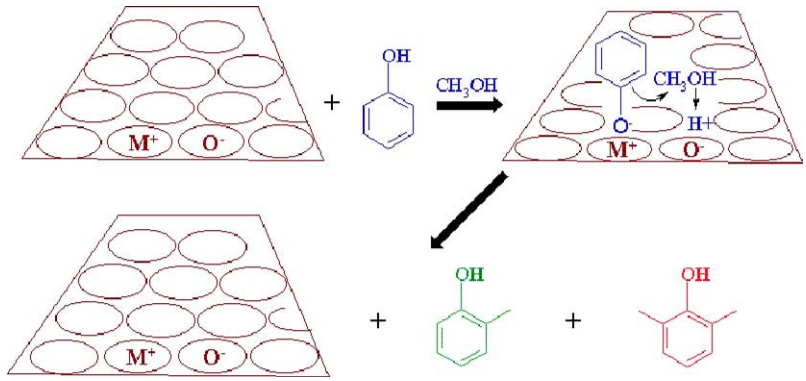

Fig. 7. A cartoonist view of mechanism for phenol methylation.

high temperatures above 573 K. This is evidenced from the disappearance of series of out-of-plane C–H overtone bands between 2050 and 1700 cm^{-1} for *ortho*-methylated phenols (Figs. 4 and 5).

4.3. Mechanism of phenol methylation on $Cu_{1-x}Co_xFe_2O_4$

IR studies clearly showed that surface-bound methoxides or strongly polarized O–H bands were formed when methanol is adsorbed on $Cu_{1-x}Co_xFe_2O_4$. Similarly phenol is dissociatively adsorbed on nearby acid–base pair sites as phenoxide ions and protons. The dissociated proton from phenol has a governing role in the fate of methanol molecules, which facilitates the formation of carbocation quite easily by protonating methanol. Thus the chemisorption of phenol on the oxides undoubtedly facilitates the protonation of methanol. It has been reported that methylation of phenol is initiated by the protonation of methanol with the aid of a Lewis acid–base pair [18] and the protonated methanol attacks the *ortho* position of phenol to form the *ortho*-methylated products.

There are two potential sites of OH groups and Lewis acid–base centers for methanol adsorption. Since the OH group of the present catalyst is incapable of protonating even strong bases like pyridine [21,50], it is highly unlikely that they could interact with methanol. Hence, Lewis acid–base sites are the most probable sites for methanol chemisorption on $Cu_{1-x}Co_xFe_2O_4$. This is true when methanol is a sole reagent. However in the presence of phenol, both methanol and phenol may compete for the same active center. Since phenol is capable of releasing proton faster, phenolate and proton adsorb relatively easily on a nearby acid–base pair site. Protons released from phenol are quite mobile and capable of protonating CH_3OH molecules leading to $CH_3^{\delta+}$ cations (Fig. 7). Thus the methanol molecule is directed to adsorb on H^+ released from phenol for methylation and hence the active center for *ortho* methylation is likely to be an acid–base pair site. An important point to be noted is that the intensity of various bands due to 2,6-xylenol decreases significantly at high temperatures ($\geqslant$ 573 K) compared to *o*-cresol and hints to a longer residence time of the latter

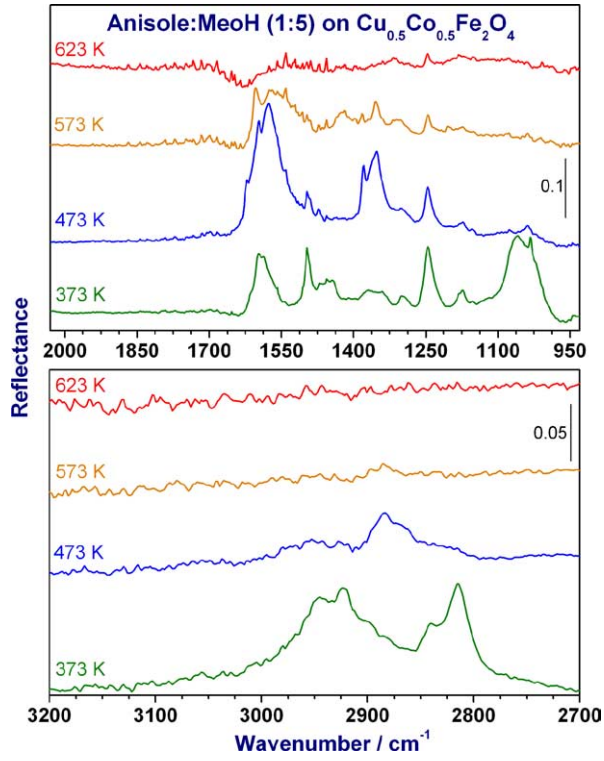

Fig. 8. Temperature-dependent FTIR spectra of anisole and methanol of 1:5 mole ratio coadsorbed on $Cu_{0.5}Co_{0.5}Fe_2O_4$ in the range of 1700–1000 cm^{-1} (top panel) and 3200–2700 cm^{-1} (bottom panel).

leading to a second *ortho* methylation which leads to the former and its fast desorption at reaction temperatures.

The above suggested phenol methylation mechanism was verified by two different experiments. Fig. 8 shows the temperature-dependent FTIR spectra of a 1:5 ratio of anisole:methanol coadsorbed on $Cu_{0.5}Co_{0.5}Fe_2O_4$. A clear domination by MeOH-derived species is evident on the catalyst surface $>$ 373 K from the bands at 2950, 2925, 2816, 1460, 1375, 1365, and 1070 cm^{-1}. Aromatic C=C stretching of anisole features observed at 1600, 1500, and 1250 cm^{-1} decreases in intensity with increasing temperature and no aromatic C–H stretching can be seen at any temperature. The above observations indicate the weak adsorption of anisole and it is opposite to PhOH + MeOH coad-

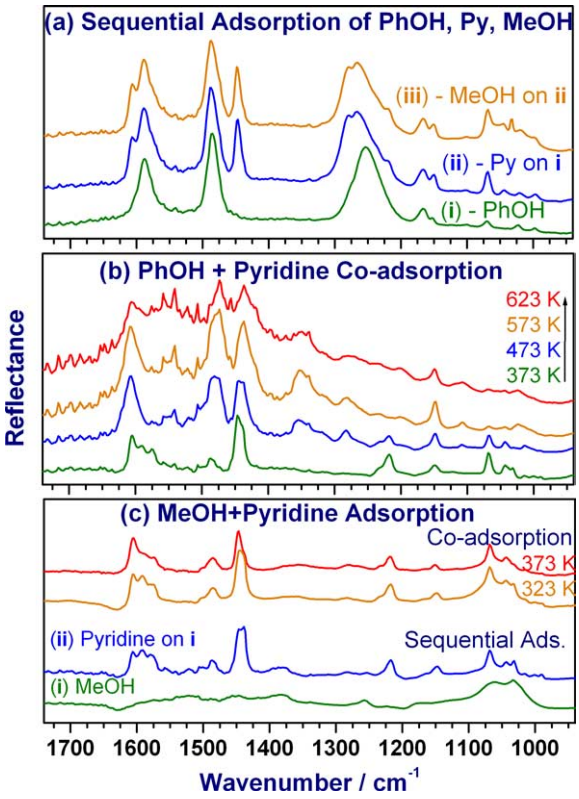

Fig. 9. FTIR spectra recorded on $Cu_{0.5}Co_{0.5}Fe_2O_4$ for competitive adsorption of reactants: (a) sequential adsorption of phenol, pyridine, and then methanol at 373 K; (b) temperature dependence of coadsorption of phenol and pyridine, and (c) sequential adsorption of methanol and pyridine at 323 K and coadsorption of methanol and pyridine at 323 and 373 K.

sorption (Fig. 6), where the surface is dominated by PhOH features. Actual catalytic reactions were carried out with a 1:5 ratio of anisole:methanol at 623 K on $Cu_{0.5}Co_{0.5}Fe_2O_4$, as described in our earlier paper for phenol methylation [19]. Neither significant anisole conversion (< 4 wt%) nor *ortho*-methylated anisole selectivity (about 1%) were observed and support the dissociative mechanism suggested for phenol methylation.

Sequential and coadsorption of reactants with acidity probe molecules of pyridine were carried out at different temperatures on $Cu_{0.5}Co_{0.5}Fe_2O_4$ to find out the competitive nature of adsorption of reactants on the surface and the results are shown in Fig. 9. Fig. 9a shows the sequential adsorption of phenol, pyridine, and then methanol at 373 K. Phenol and pyridine features coexist after pyridine exposure to a phenol-adsorbed surface; however, hardly any methanol features are seen with subsequent methanol adsorption. Fig. 9b shows the coadsorption of a 1:1 ratio of phenol and pyridine at 373 K and at higher temperatures. The catalyst surface is clearly dominated by pyridine features at 373 K; however, phenol features are also seen at 1595, 1587, and 1230 cm^{-1}. At 473 K phenol features decrease in intensity, and a feature at 1540 cm^{-1} appears and increases in intensity $\geqslant$ 473 K is due to pyridinium ions [21] and supports the dissociative mechanism of phenol methylation. The above results also indicate that the pyridine and phenol are equally competing for the adsorption sites when adsorbed sequentially, but pyridine competes at a higher level in the case of coadsorption.

Fig. 9c shows both the sequential and the coadsorption of methanol and pyridine. Sequential adsorption of methanol and pyridine carried out at 323 K clearly demonstrates the initially adsorbed methanol is displaced fully by pyridine. Coadsorption of a 1:1 ratio of methanol and pyridine also shows that there is hardly any methanol features and is dominated by pyridine features $\leqslant$ 373 K. This result demonstrates that the weakly acidic methanol can be displaced easily by strongly adsorbing pyridine. The weak methanol features in Figs. 6 (phenol + methanol) and 9c (pyridine + methanol) clearly support the phenol methylation reaction mechanism and justifies the strong domination of the catalyst surface by phenol. The above results also indicates that despite the high methanol content in the phenol methylation feed, on the catalyst surface it may be close to a 1:2 ratio of phenol:methanol and also supports the reaction stoichiometry. A large amount of MeOH in the reaction mixture was necessary due to the above weak interaction of MeOH to the catalyst surfaces.

C-alkylation can take place either by a direct route or by the isomerization of O-alkylation product. To decide between these two routes, anisole was passed over the catalyst under optimum reaction conditions [19,50]. No isomerized products (cresols) were obtained. Thus these compounds do not have any activity for the transformation of anisole into *o*-cresol in the catalytic conversion of anisole at 623 K. It may be noted that this is in contrast to the behavior of alumina, on which alkyl phenyl ethers undergo isomerization to C-alkyl phenols [6].

5. Conclusions

The present work describes the FTIR adsorption of reactants and products of phenol methylation on $Cu_{1-x}Co_x$-Fe_2O_4. FTIR adsorption of methanol on $Cu_{1-x}Co_xFe_2O_4$ indicates a dissociative chemisorption of CH_3OH to methoxylation as well as oxidation of methanol even at 373 K. As the temperature increases, methoxylated species were progressively converted into formaldehyde, formate, and dioxymethylene species, and above 573 K complete oxidation takes place to CO, CO_2, and H_2. Methoxy and formate species are comparatively unstable on Cu-containing samples due to the presence of easily reducible Cu^{2+} ion.

IR studies of phenol adsorption on $Cu_{1-x}Co_xFe_2O_4$ show signals of both undissociated phenol and phenolate-like species. Phenolate species are formed due to dissociative adsorption of phenol on an acid–base pair site. Chemisorbed phenol molecules are adsorbed through oxygen atoms to the Lewis acid sites with aromatic rings perpendicular to the plane of the oxide. Aromatic rings of methylated phenols also interact in a very similar manner and out-of-plane C–H

vibrations are observed supporting this point. Also it is found that methylated phenols have weak interaction with the surface in comparison with phenol and are highly susceptible to desorbing from the surface as the temperature increases and thus facilitate efficient methylation on $Cu_{1-x}Co_xFe_2O_4$ system.

It is found that methylation of phenol is initiated by the protonation of methanol with the aid of a Lewis acid–base pair. The protonation of methanol occurs on the oxides by accepting protons released from the adsorbed phenol and the protonated methanol attacks the *ortho* position of phenol to form the *ortho*-methylated products. Thus the active center for the *ortho* methylation is an acid–base pair site. This mechanism is further supported by the IR studies of competitive adsorption of reactants with acidity probe molecules and coadsorption of anisole + methanol. Activation of methanol requires relatively high temperatures on $CoFe_2O_4$ indicating the necessity of relatively high temperatures to achieve high phenol methylation. This information corroborates our earlier finding that $CoFe_2O_4$ requires 648–673 K whereas for Cu-containing samples only 623 K is required for high phenol conversion [19].

Acknowledgments

The authors thank the reviewer for constructive suggestions on earlier version of this manuscript. T.M., M.V., and S.P. thank the Council of Scientific and Industrial Research (CSIR), New Delhi, for a senior research fellowship.

References

[1] K. Weissermel, H.J. Arpe, Industrial Organic Chemistry, Verlag Chemie, Weinheim, 1978, p. 316.
[2] H. Fiege, H.-W. Voges, in: B. Elvers, S. Hawkins, G. Schulz (Eds.), Ullman's Encyclopedia of Industrial Chemistry, VCH, Weinheim, 1991, p. 313, A19.
[3] G.L. Warner, US patent 4933509 (1990).
[4] R.A. Battista, J.G. Bennett, J.J. Kokoszka, F.L. Tungate, US patent 4661638 (1987).
[5] K. Tanabe, T. Nishizaki, in: G.C. Bond, P.B. Wells, F.C. Thompkins (Eds.), Proc. 6th Internat. Congr. Catal., London, 1977, p. 863.
[6] M. Inoue, S. Enomoto, Chem. Pharm. Bull. 20 (1972) 232.
[7] S. Balsama, P. Beltrame, P.L. Beltrame, P. Carniti, L. Forni, G. Zuretti, Appl. Catal. 13 (1984) 161.
[8] V. Venkatrao, K.V.R. Chary, V. Durgakumari, S. Narayanan, Appl. Catal. 61 (1990) 89.
[9] S. Sato, K. Koizumi, F. Nozaki, J. Catal. 178 (1998) 264.
[10] P. Beltrame, P.L. Beltrame, P. Carniti, A. Castelli, L. Forni, Appl. Catal. 29 (1987) 327.
[11] F.M. Bautista, J.M. Campelo, A. Garcia, D. Luna, J.M. Marinas, A. Romero, J.M. Navio, M. Macias, Appl. Catal. A 99 (1993) 161.
[12] S. Velu, C.S. Swamy, Appl. Catal. A 119 (1994) 241.
[13] H. Grabowska, J. Jablonski, W. Mista, J. Wrzyszc, Res. Chem. Intermed. 22 (1996) 53.
[14] M. Misono, N. Nojiri, Appl. Catal. 64 (1990) 1.
[15] B.E. Leach, US patent 4227024 (1980).
[16] T. Kotanigawa, M. Yamamoto, K. Shimakowa, Y. Yoshida, Bull. Chem. Soc. Jpn. 44 (1971) 1961.
[17] T. Kotanigawa, K. Shimakowa, Bull. Chem. Soc. Jpn. 47 (1974) 1535.
[18] T. Kotanigawa, Bull. Chem. Soc. Jpn. 47 (1974) 950.
[19] T. Mathew, N.R. Shiju, K. Sreekumar, B.S. Rao, C.S. Gopinath, J. Catal. 210 (2002) 405;
T. Mathew, S. Shylesh, B.M. Devassy, C.V.V. Satyanarayana, B.S. Rao, C.S. Gopinath, Appl. Catal. A 261 (2004) 292;
T. Mathew, B.S. Rao, C.S. Gopinath, J. Catal. 222 (2004) 107.
[20] K. Lázár, T. Mathew, Z. Koppány, J. Megyeri, V. Samuel, S.P. Mirajkar, B.S. Rao, L. Guczi, Phys. Chem. Chem. Phys. 4 (2002) 3530.
[21] T. Mathew, N.R. Shiju, B.B. Tope, S.G. Hegde, B.S. Rao, C.S. Gopinath, Phys. Chem. Chem. Phys. 4 (2002) 4260.
[22] T. Mathew, N.R. Shiju, R.Y. Nimje, P.M. Adkine, B.S. Rao, V.V. Bokade, Chem. Eng. Res. Design, Part A 81 (2003) 265.
[23] G. Busca, V. Lorenzelli, J. Catal. 66 (1980) 155.
[24] G. Busca, A.S. Elmi, P. Forzatti, J. Phys. Chem. 91 (1987) 5263.
[25] K. Nakamoto, Infrared Spectra of Inorganic and Coordination Compounds, Wiley, New York, 1963, p. 199.
[26] G. Busca, P.F. Rossi, V. Lorenzelli, M. Benaissa, J. Travert, J.C. Lavalley, J. Phys. Chem. 89 (1985) 5433.
[27] G. Busca, P. Forzatti, J.C. Lavalley, E. Tronconi, in: B. Imelik, et al. (Eds.), Catalysis by Acids and Bases, Elsevier, Amsterdam, 1985, p. 14.
[28] N. Takezawa, J. Chem. Soc., Chem. Commun. (1971) 1451.
[29] Y. Noto, K. Fukuda, T. Onishi, K. Tamaru, Trans. Faraday Soc. 63 (1967) 2300.
[30] A. Ueno, T. Onishi, K. Tamaru, Trans. Faraday Soc. 66 (1970) 756.
[31] G. Munuera, J. Catal. 18 (1970) 19.
[32] E.W. Thornton, P.G. Harrison, J. Chem. Soc., Faraday Trans. I 71 (1975) 2468.
[33] M.A. Natal-Santiago, J.A. Dumesic, J. Catal. 175 (1998) 252.
[34] L.J. Burcham, I.E. Wachs, Catal. Today 49 (1999) 467.
[35] L.J. Burcham, G. Deo, X. Gao, I.E. Wachs, Top. Catal. 11/12 (2000) 85.
[36] The Aldrich Library of FTIR spectra, vol. 1, 2nd ed., 1997, Spectrum No. 15,490-3, p. 160.
[37] C. Chauvin, J. Saussey, J.C. Lavalley, H. Idriss, J.-P. Hindermann, A. Kiennemann, P. Chaumette, P. Courty, J. Catal. 121 (1990) 56.
[38] A.A. Davydov, W.M. Shchekochikhin, P.M. Zajcev, Y.M. Shchekochikhin, P. Keier, Kinet. Katal. 12 (1971) 694.
[39] E.B. Wilson, Phys. Rev. 45 (1934) 706.
[40] J.H.S. Green, J. Chem. Soc. (1961) 2236.
[41] D.R. Taylor, K.H. Ludlum, J. Phys. Chem. 76 (1972) 2882;
R. Sokoll, H. Hobert, J. Catal. 125 (1990) 285;
S. Scire, C. Crisafulli, R. Maggiore, S. Minico, S. Galvagno, Appl. Surf. Sci. 93 (1996) 309.
[42] M.I. Tejedor-Tejedor, E.C. Yost, M.A. Anderson, Langmuir 6 (1990) 979.
[43] L. Palmisano, M. Schiavello, A. Sclafani, G. Martra, E. Borello, S. Coluccia, Appl. Catal. B 3 (1994) 117.
[44] R.O. Kagel, R.G. Greenler, J. Chem. Phys. 49 (1968) 1638.
[45] G. Karagounis, O. Peter, Z. Elektrochem. 61 (1957) 827.
[46] G. Karagounis, O. Peter, Z. Elektrochem. 61 (1957) 1094.
[47] S. Scire, C. Crisafulli, R. Maggiore, S. Minico, S. Galvagno, Appl. Surf. Sci. 93 (1996) 309.
[48] The Aldrich Library of FTIR spectra, vol. 2, 2nd ed., 1997, Spectrum No. 12,322-6, p. 160.
[49] M. Vijayaraj, C.S. Gopinath, J. Catal. 226 (2004) 230.
[50] T. Mathew, Synthesis and characterization of mixed oxides containing cobalt, copper and iron and study of their catalytic activity, Ph.D. thesis, University of Pune (2002).